Studies on Highly Dense Pure YIG Polycrystalline Ceramics Fabricated by Tape-casting Method

Chong Zhao
Renmin University of China
Yingkui Li
Songshan Lake Materials Laboratory
Xiaofei Shen
Songshan Lake Materials Laboratory
Zhijun Cao
University of Virginia
Zhiquan Cao
New York University
Zicheng Wen
Songshan Lake Materials Laboratory
Xuanyi Yuan
Renmin University of China
Chaoyang Ma
Songshan Lake Materials Laboratory
Yongge Cao (caoyongge@sslab.org.cn)
Songshan Lake Materials Laboratory, Dongguan 523808, Guangdong, China Institute of Physics, Chinese Academy of Sciences, Beijing 100190, China

Research Article

Keywords: YIG ceramics, tape-casting, microwave, hysteresis loss, magnetodielectric ceramics

Posted Date: August 12th, 2020

DOI: https://doi.org/10.21203/rs.3.rs-57431/v1

Studies on highly dense pure YIG polycrystalline ceramics fabricated by tape-casting method

Chong Zhao[a], Yingkui Li[b], Xiaofei Shen[b], Zhijun Cao[c], Zhiquan Cao[d], Zicheng Wen[b,e], Xuanyi Yuan[a], Chaoyang Ma[b,*], Yongge Cao[b,e,*]

[a] Department of Physics, Renmin University of China, Beijing 100872, China

[b] Songshan Lake Materials Laboratory, Dongguan 523808, Guangdong, China

[c] University of Virginia, Charlottesville, VA 22904, USA

[d] New York University, New York, NY 10003, USA

[e] Institute of Physics, Chinese Academy of Sciences, Beijing 100190, China

*Corresponding authors: caoyongge@sslab.org.cn

machaoyang@sslab.org.cn

Abstract

Pure phase $Y_3Fe_5O_{12}$ (YIG) ceramics was successfully produced by tape-casting forming process and one-step solid-state reaction method. With the sintering temperature above 1100 ℃, the pure phase YIG ceramics was synthesized with no YIP or Fe_2O_3 phase in XRD patterns. YIG ceramic sintering at 1400 ℃ for 10 h showed a clear grain structure with an obvious grain boundary, and no pores were observed in the SEM images. YIG ceramics in this paper has a high relative density which was 99.8% and the saturation magnetization was 28.2 emu/g at room temperature. The hysteresis loss at temperatures of 230-360 K was smaller than 10 mJ/kg. The $\tan\delta_\varepsilon$ was nearly zero at 6~7 GHz and 11~12 GHz, showing that it can be used as a good material for microwave applications. In

addition, the low values of $\tan\delta_\varepsilon$ and $\tan\delta_\mu$ indicates that it may have a good electromagnetic wave absorption ability.

Keywords

YIG ceramics; tape-casting; microwave; hysteresis loss; magnetodielectric ceramics

1. Introduction

Yttrium iron garnet, $Y_3Fe_5O_{12}$ (YIG) has a bcc cubic structure and belongs to the space group *Ia-3d* (230). Furthermore, per unit cell (1895.6 $Å^3$) contains 8 formula units, where Y^{3+} ions occupy the eight-coordinate (O^{2-}) dodecahedral sites, while Fe^{3+} ions partially take up six-coordinate octahedral and three-coordinate tetrahedral sites. YIG materials and its modifications by doping as soft ferrites are suitable for magnetic microwave devices with high frequency and low microwave loss [1,2]. Microwave filters and oscillators based on YIG have a wider electric tuning range in frequency than other candidates including ferroelectric and varactors [3]. Multiferroic magnetoelectric materials developed on YIG exhibit both ferroelectricity and ferromagnetism, and typically yield much larger magnetoelectric coupling response than natural multiferroic single-phase compounds, making them suitable for magneto-electric applications [4]. Faraday rotators with substituted YIG films or bulk crystals own large Faraday Rotation capacity, low saturation magnetization and low optical absorption loss, showing high potential applications in magneto-optical devices [5,6].

Pure polycrystalline Bi-substituted YIG thin films were grown on Corning glass substrates by an original CVD technique and its Faraday rotation properties were studied [7]. Bi-substituted Y-Yb mixed iron garnet single crystals were grown by the flux method and the specific Faraday Rotation, optical absorption coefficient and the

saturation magnetization were investigated [5]. Nowadays, polycrystalline YIG (powder or bulk ceramic) are generally synthesized through conventional solid-state reaction (CSSR) method. For YIG ceramics, properties of density, purity and microstructure have great impact on the magnetic properties and therefore the performance of its microwave devices. However, some secondary phases (Fe_2O_3, $YFeO_3$, YFe_2O_4) are usually coexisted with YIG fabricated by CSSR method [8,9]. The growth kinetic and reaction mechanism of Y_2O_3-Fe_2O_3 system were studied by different diffusion couples. And, the results showed that the formation of YIG phases were highly depended on pre-formed YIP phases and the diffusion of Fe^{3+} cations [10-12]. By adding excess 8-10 wt% Fe_2O_3, 99% of YIG ceramic phase was achieved. What's more, YIG with properly excess Fe_2O_3 could be used for high frequency tunable dielectric resonator antenna (DRA) [13,14]. Recently, YIG ceramics with about 98-99% of theoretical density were fabricated by solid-state reaction method [15,16]. While, new fabrication methods are pursued for much higher dense and purity fine-grained YIG ceramics.

In this work, high-dense pure YIG polycrystalline ceramics were fabricated by tape-casting forming process and one-step solid-state reaction method. Phase purity, relative density and micro-morphology depends on sintering temperature and holding time were studied. The activation energy was calculated from the linear Arrhenius plots. XPS was performed to check valance states of Fe and O atoms, as well as EPR spectrum was introduced to check O vacancy. Thereafter, magnetic and dielectric properties were chractarized for the sample sintered at 1400 ℃ for 8h.

2. Material and methods

Commercially available powders of Y_2O_3 (99.99%) and Fe_2O_3 (99.99%) were used as raw materials without further purifying. Powders were precisely weighted in accordance with

the stoichiometry of $Y_3Fe_5O_{12}$ and then added into the mixed solvent of ethanol and xylene. Besides, proper amount of TEOS (Tetraethyl Orthosilicate) as sintering aid and fish oil as dispersant were put into the mixture. Then, the mixed slurry was planetary ball-milled for 24 h. Subsequently, some binder (Polyvinyl Butyral), plasticizers (Polyalkylene Glycol & Butyl Benzyl Phthalate) and defoamers (n-butyl alcohol & ethylene glycol) were added and ball-milled for another 24 h.

Thereafter, the tape-casting forming process was carried out. The distance between the blade and tape was 500 μm and the casting speed was 500 mm/min. The prepared slurry on the tape was dried at room temperature, and then cut into slices. A proper number of layers of slices were stacked and compressed under 20 Mpa at 120 ℃ to form into green body. The green body was calcined at 800 ℃ in an oxygen atmosphere to remove organic additives, and then sintered at various temperatures in a furnace under air atmosphere. Finally, the obtained YIG ceramics were prepared for characterization.

The phase identification of the fabricated ceramics was performed on an XRD system (Bruker, Germany) using Cu *Kα* radiation (λ=1.5406 Å). The surface micro-morphology was carried on a field-emission SEM (JSM-6700F, JEOL, Japan). The XPS was conducted by using an X-ray photoelectron spectrometer (ESCALAB 250X, Thermo Scientific, USA). The EPR was conducted by using an electron paramagnetic resonance instrument (A300-10/12, Bruker, Germany). The bulk density was measured using the Archimedes' method. The magnetic hysteresis loops were obtained by a vibrating sample magnetometer (VSM, QD, USA). The magnetic and dielectric properties were determined with a microwave network analyzer (PNA-N5244A, Agilent, USA).

3. Results and discussion

3.1. XRD

Fig. 1 shows the XRD patterns of YIG ceramics fabricated by combining tape-casting forming process and solid-state reaction method at various sintering temperatures in air atmosphere. It can be clearly observed that the ceramics with sintering temperatures above 1100 ℃ are all YIG pure phases (PDF# 71-2150). According to Ali's report, YIG ceramics prepared through dry-pressing forming process generally contain unwanted phase of YIP even with 1250 ℃ sintering temperature [10]. It is suggested that YIP is formed as an intermediate phase and will further react with Fe_2O_3 to produce single-phase YIG by diffusion process [12]. It is suggested that Fe^{3+} cations diffuse and initiate the Fe-Y atomic bonding. Then, with Fe^{3+} cations continuously diffusing, the YIP layer covered on the surface of Y_2O_3 particles turned to be YIG while the inner Y_2O_3 changed into YIP. Considering the saturated vapor pressure of Fe and Y calculated by Eq. (1) and listed in Table 1, it can be seen that Fe has a larger saturated vapor pressure than Y, which signifies that the iron is more volatile in this system. If Fe_2O_3 is inhomogeneous in this system, high concentration of Fe element means more evaporation at high temperature. So, the existence of YIP impurity is highly depended on the inhomogeneous and evaporation of Fe_2O_3. Compared with dry-pressing forming method, our tape-casting forming method provide much better homogeneous mixture of Y_2O_3 and Fe_2O_3 particles, thus leading to the highly pure YIG ceramics.

$$\log(p/atm) = A + B/T + C * \log(T) + D/T^3 \qquad (1)$$

Here, coefficients in the equation can be obtained from reference [17] and listed in Table 1.

Table 1. Vapor pressure of metallic elements Fe and Y in the solid state at about 1800 K.

Element	A	B	C	D	T(melt)/K	P/atm
Fe	7.1	-21723	0.4536	-0.5846	1808	3.652×10^{-4}

Y	9.735	-22306	-0.8705	0	1799	2.967×10^{-6}

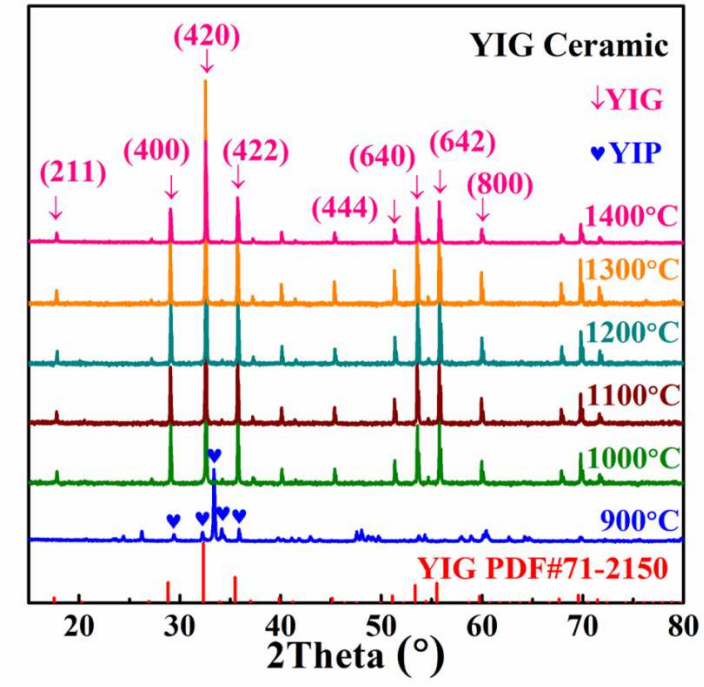

Fig. 1. The XRD patterns of YIG ceramics sintered under various temperatures in air atmosphere.

3.2. SEM and XPS

Figs. 2(a-f) show the SEM images of YIG ceramics prepared at various sintering temperatures for 10 h and the evolution of morphologies is in accord with Ostwald ripening process. Along with the sintering temperature increasing from 900 to 1400 ℃, driven by the sintering kinetics, little grains gradually adhere to each other with grain boundaries and grow to be big grains to reduce the interfacial area, as a result, gaps and pores between grains are gradually eliminated at the same time. Samples sintered at 1400 ℃ exhibit no pores existed in both grains and boundaries, indicating a quite high densification, as

discussed in Section 3.3. Grain size in Fig. 4(f) is non-uniform and varies from several microns to several dozens of microns, which can be ascribed to the asynchronous growth of grains at different regions and thereof migration of grain-boundaries, as shown in Figs. 2(a-e).

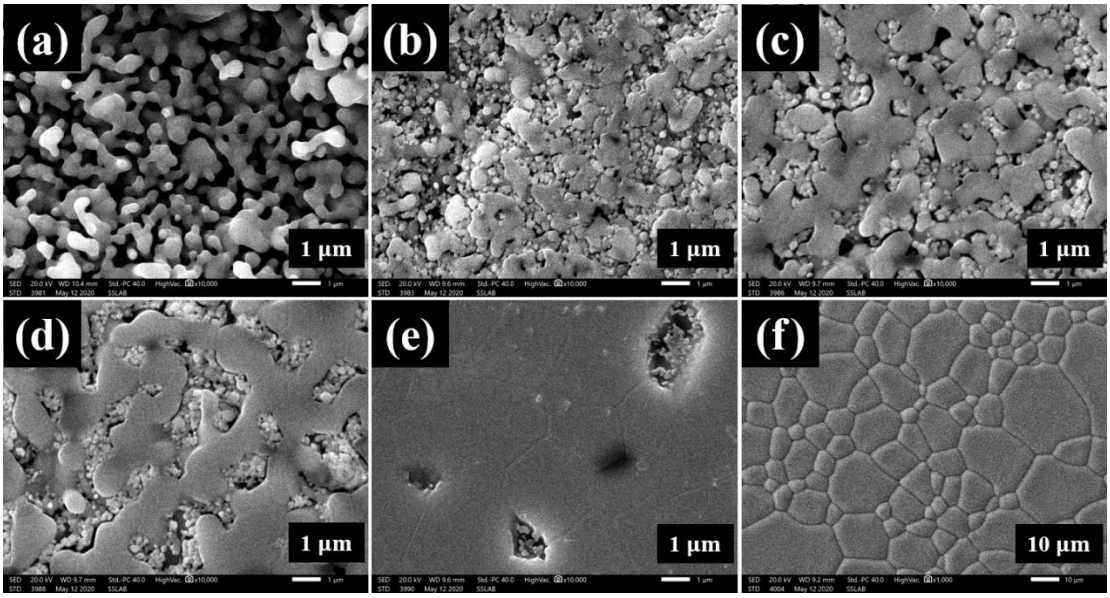

Fig. 2. SEM images of YIG ceramics sintered at (a) 900 ℃, (b) 1000 ℃, (c) 1100 ℃, (d) 1200 ℃, (e) 1300 ℃ and (f) 1400 ℃ for 10 h.

According to Chen's report, Fe^{2+} ions and oxygen vacancies may exist in ceramics fabricated by high temperature sintering process due to the low oxygen conditions [16], and this can be verified by XPS measurement. Fig. 3 shows XPS spectra of YIG ceramics sintered at 1400 ℃ for 10 h. The XPS spectrum confirmed the existence of Fe $2p_{1/2}$, Fe $2p_{3/2}$, Fe 3s, Fe 3p, O 1s, O 2s, Y 3s, Y $3p_{1/2}$, Y $3p_{3/2}$, C 1s, Y 3d, Y 4s and Y 4p signals for the sample as shown in Fig 3(a). In Fig. 3(b), based on the Lorentzian-Gaussian fitting, Fe $2p_{3/2}$ peak and Fe $2p_{1/2}$ peak can both be divided into Fe^{3+} and Fe^{2+} peaks which are centered at 711.6 eV, 726.4 eV, 710.2 eV and 724.2 eV. Meanwhile, O 1s spectrum in Fig. 3(c) was divided into two peaks centered at 529.9 eV and 531.6 eV. And the latter peak

indicated the existence of oxygen vacancy which can also be proved by the EPR spectrum, as shown in the illustration in Fig. 3(c).

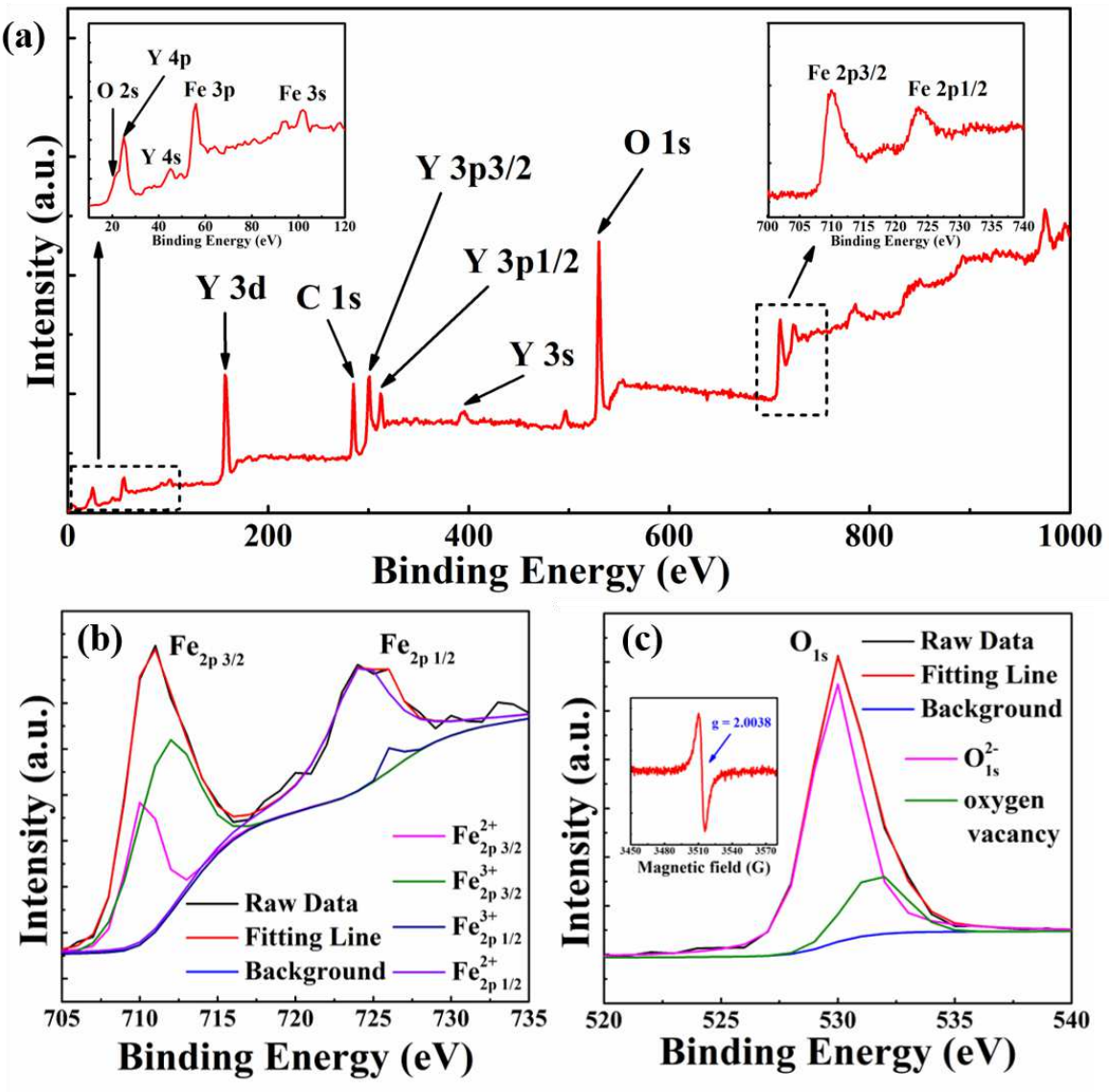

Fig. 3. XPS spectra in (a) the survey range, (b) Fe ion and (c) O ion in YIG ceramics sintered at 1400 ℃ for 10 h.

3.3. Relative density and activation energy

The sintering kinetics, namely densification kinetics, of YIG ceramics could be characterized by the relationship between the relative density and sintering conditions (temperatures and holding times). Densities of YIG ceramics sintered at various

temperatures and holding times were measured by Archimedes' method and were plotted in Fig. 4(a). Obviously, higher sintering temperature and longer holding time did lead to higher relative density. Besides, the relative density increased significantly along with the temperature below 1375 ℃, while it increased slowly when the temperature further raised. For samples sintered at 1450 ℃ for 8 h, the relative density reached the highest value of 99.8%, which was bigger than that values reported in references [15] and [18]. The high relative density indicated extremely low residual porosity and highly dense microstructure. Densification kinetics can be interpreted by Arrhenius equation: [10,18,19]

$\ln K = -E_a/RT + C$

where, E_a is the activation energy for YIG ceramic densification, R is the gas constant (8.314 J/mol/K), T is the absolute temperature, C is the constant, and K is the rate constant depending on temperature. Densification rate versus reciprocal temperature was plotted in Fig. 4(b), where rate constant K was related to relative density and calculated from Fig. 4(a). By linear fitting, the value of E_a was determined to be 183.81 kJ/mol, which was comparable with the activation energy of 169 kJ/mol for lattice diffusion or grain boundary formation [18] and much smaller than the energy of 484 kJ/mol for YIG formation from YIP [10]. It can be drawn that the mechanism of YIG phase formation and ceramics densification was the result of homogeneous diffusion probably assisted by the sintering aids of SiO_2 (products of TEOS decomposition) located at grain boundaries.

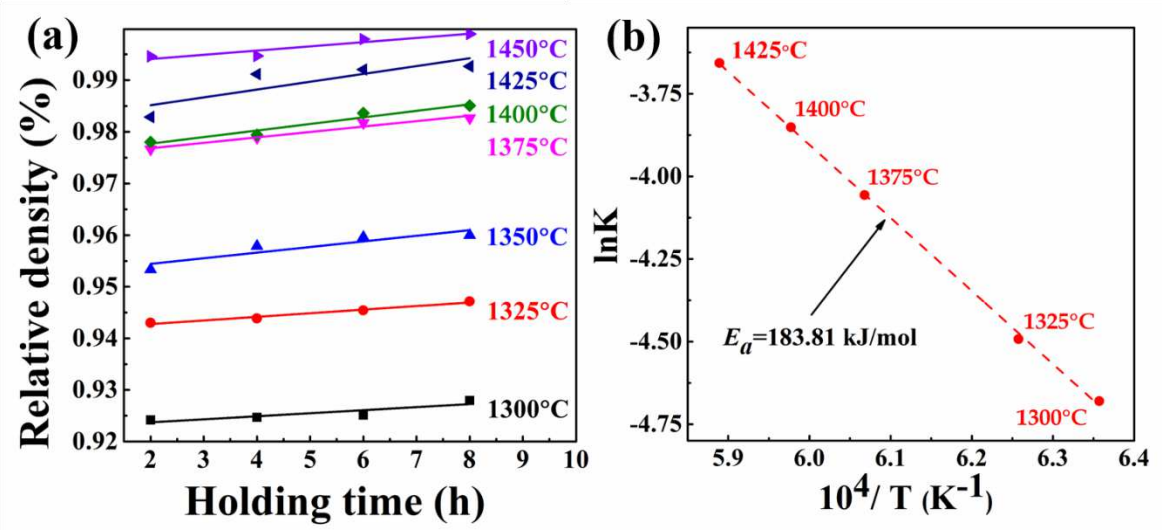

Fig. 4. (a) Relative densities of YIG ceramics sintered at various temperatures and holding times. (b) The activation energy analysis for YIG ceramics.

3.4. Intrinsic magnetic property

The magnetic properties of YIG ceramics sintered at 1400 ℃ were studied by the static hysteresis loops under various temperatures, as shown in Fig. 5(a). The well-defined hysteresis loop can be clearly observed at 30 K, while turned to be narrower along with the increase of temperature. The saturation magnetization (M_s) and hysteresis loss (area of the hysteresis loop) depending on temperature were plotted in Fig. 5(b). The value of M_s decreased from 38.9 emu/g down to 25.3 emu/g as the temperature increased from 30 K up to 360 K. And, the trend could be ascribed to the enhanced thermal vibrations of atoms and lattices under high temperatures, and hence magnetic dipoles were difficult to be aligned [20]. It was worth mentioning that the room-temperature (300 K) value of M_s was 28.2 emu/g, which was a little higher than that value (27.4 emu/g) reported in previous literature [15]. The result indicated that our YIG ceramics exhibited much higher relative density and more compact microstructures. Hysteresis loss, characterized by the area of the hysteresis loop, generally decreased with temperature. However, in this work, there was an upturn

point at 230 K (4 mJ/kg), and the mechanism needed to be further studied. Besides, hysteresis loss at 30 K was as high as 238.8 mJ/kg, while values of that at temperatures of 230-360 K was smaller than 10 mJ/kg.

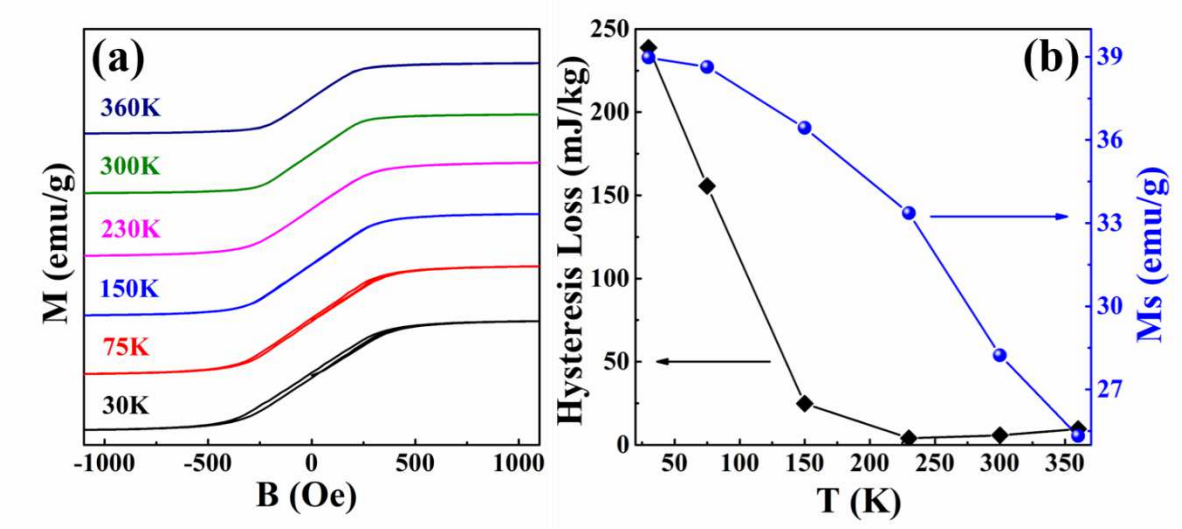

Fig. 5. (a) Magnetic hysteresis loops and (b) M_s and hysteresis loss of YIG ceramics sintered at 1400 ℃ for 8 h at various test temperatures.

3.5. Electromagnetic parameters

Fig. 6 shows zero-field complex permittivity properties of home-made YIG ceramic circle (the fabricated YIG ceramics were grinded into powder, homogenously mixed with paraffin by a mass ratio of 3:7, and thereafter formed into a 2 mm thick circle with an inner diameter of 3 mm and an outer diameter of 7 mm). Along with the frequency increasing from 2 to18 GHz, the changing trend of real part ε' (the ability for the storage of electrical energy) and the imaginary part ε'' (the dissipation capacity of electrical energy) is just the opposite, and some relaxation peaks are clearly observed as a result of multiple relaxation processes, as shown in Fig.6 (a). [21] In addition, the dielectric loss tangent $\tan\delta_\varepsilon$ determined by $\varepsilon''/\varepsilon'$ fluctuates with the frequency, and interestingly, $\tan\delta_\varepsilon$ at about 6~7 GHz and 11~12 GHz is extremely low suitable for practical microwave devices, as shown

in Fig. 6(b). As we know, the dielectric loss is ascribed to conduction loss and polarization relaxation loss. And, polarization relaxation loss can be characterized by the Cole-Cole semicircle, that is, a simple semicircle in the $\varepsilon'\varepsilon''$-coordinate plane means a polarization relaxation process. As shown in Fig. 6(c), there are three semicircles suggesting that the dielectric loss is determined by multiple dielectric relaxation losses, and this result is in accordance with relaxation peaks in Fig. 6(a). [22] Future work will be focused on dielectric properties of YIG ceramics under applied magnetic field in a wide range of frequency.

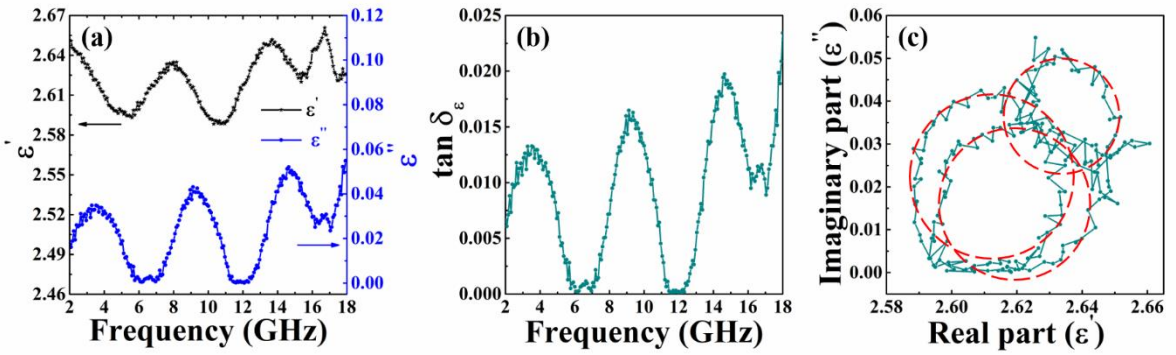

Fig. 6. Frequency dependence of (a) ε' and ε'', (b) tanδ_ε, and (c) Cole-cole semicircle of YIG ceramics sintered at 1400 ℃ for 8 h.

For complex permeability, the real part μ' (the ability for the storage of magnetic energy) and the imaginary part μ'' (the dissipation capacity of magnetic energy) have the same changing trend along with the rise of frequency from 2 to 18 GHz, as shown in Fig. 7(a). Apparently, μ' and μ'' exhibit three distinct resonance peaks located at about 6.2 GHz, 11.6 GHz and 16.6 GHz in turn, meaning perfect magnetic loss ability at these frequencies, which is well agree with the result of magnetic loss tangent tanδ_μ determined by μ''/μ', as shown in Fig. 7(b). Generally, the magnetic loss contains exchange resonance, natural resonance and eddy current loss in the investigated frequency from 2 GHz to 18 GHz.

According to previous report, if the eddy current loss is the only reason for the magnetic loss, frequency dependence of $C_0 = \frac{\mu''}{\mu'^2 f}$ should be a constant. [23] In Fig. 7(c), C_0 is nearly constant with little fluctuations at the range of 5~18 GHz, suggesting that the eddy current loss dominates the magnetic loss but also the exchange resonance may exist. As for lower frequency between 2 GHz and 5 GHz, the natural resonance will always dominate. The electromagnetic wave (EMW) dissipation is both rely on the dielectric loss and magnetic loss. For our YIG ceramics, values of $\tan\delta_\varepsilon$ and $\tan\delta_\mu$ were pretty low, indicating that this material may have a good EMW absorption ability, on which future work will be focused.

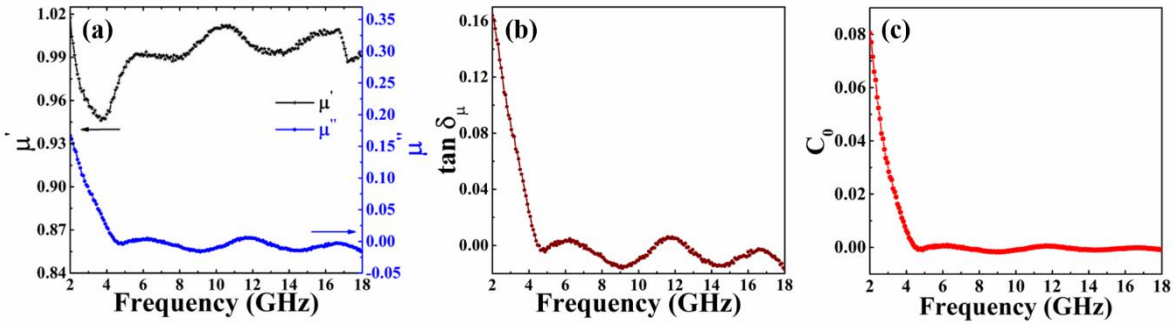

Fig. 7. Frequency dependence of (a) μ' and μ'', (b) $\tan\delta_\mu$, (c) C_0 of YIG ceramics sintered at 1400 ℃ for 8 h.

4. Conclusion

In this study, pure phase YIG ceramics were successfully produced by tape-casting forming process and one-step solid-state reaction method. The microstructure of the YIG ceramics sintering at 1400 ℃ for 10 h showed a clear grain structure with an obvious grain boundary, and no pores were observed in the SEM images. At 1450 ℃ with a holding time of 8 h, the relative density of the YIG ceramic was nearly 99.8%. The activation energy was calculated to be 183.81 kJ/mol. The saturation magnetization was 28.2 emu/g at 300 K.

And, hysteresis loss at 30 K was as high as 238.8 mJ/kg, while values of that at temperatures of 230-360 K was smaller than 10 mJ/kg. The $\tan\delta_\varepsilon$ was nearly zero at 6~7 GHz and 11~12 GHz. The low values of $\tan\delta_\varepsilon$ and $\tan\delta_\mu$ indicates that it may have a good electromagnetic wave absorption ability. This work provided a new fabrication method for much higher dense and purity fine-grained YIG ceramics. And the future work will be focused on the study of the uptown point (230 K) on the hysteresis loss chart, the dielectric properties under applied magnetic field in a wider range of frequency and the EMW absorption of the dense YIG ceramics.

Acknowledgments

This work was supported by the National Key R&D Program of China (2017YFB0403200) and the National Nature Science Foundation of China (No. 51872327).

References

[1] R. Valenzuela, Magnetic ceramics, Cambridge University Press, New York, 1994.

[2] D. Badahur, Current Trends in Applications of Magnetic Ceramic Materials, B. Mater. Sci. 15 (1992) 431-439.

[3] J.D. Adam, L.E. Davis, G.F. Dionne, E.F. Schloemann, S.N. Stitzer, Ferrite devices and materials, IEEE T. Microw. Theory. 50 (2002) 721-737.

[4] C. Nan, M.I. Bichurin, S. Dong, D. Viehland, G. Srinivasan, Multiferroic magnetoelectric composites: Historical perspective, status and future directions, J. App. Phys. 103 (2008) 031101.

[5] M. Huang, S.Y. Zhang, Growth and characterization of rare-earth iron garnet single crystals modified by bismuth and ytterbium substituted for yttrium, J. Mater. Chem. Phys. 73 (2002) 314-317.

[6] M. Huang, Z.C. Xu, Liquid phase epitaxy growth of bismuth-substituted yttrium iron garnet thin films for magneto-optical applications, Thin Solid Films, 450 (2004) 324–328.

[7] J.L. Deschanvres, M. Langlet, B. Bochu, J.C. Joubert, Growth of Bi-substituted YIG thin films for magneto-optic applications, J. Magn. Magn. Mater. 101 (1991) 224-226.

[8] N. Kimzuka, T. Katsura, Standard free energy of formation of $YFeO_3$, $Y_3Fe_5O_{12}$ and a new compound YFe_2O_4 in the Fe_2O_3-Y_2O_3 system at 1200 ºC, J. Solid State Chem. 13 (1975) 176-181.

[9] F. Sánchez-De Jesús, C.A. Cortés, R. Valenzuela, S. Ammar, A.M. Bolarín-Miró, M. Bolarin-Miro, Synthesis of $Y_3Fe_5O_{12}$ (YIG) Assisted by High-energy Ball Milling, Ceram. Int. 38 (2012) 5257-5263.

[10] W.F.F.W. Ali, M. Othman, M.F. Ain, N.S. Abdullah, Z.A. Ahmad, The Investigation of the Phenomenological YIG Phase Formation Within 1000 ºC to 1250 ºC: A Kinetic Approach, J. Am. Ceram. Soc. 99 (2015) 315-323.

[11] V. Buscaglia, F. Caracciolo, C. Bottino, M. Leoni, P. Nanni, Reaction diffusion in the Fe_2O_3-Y_2O_3 system, Acta Mater. 45 (1997) 1213-1224.

[12] A. Sztaniszláv, E. Sterk, L. Fetter, M. Farkas-Jahnke, J. Lábár, Investigation of garnet formation by sintering of Y_2O_3 and Fe_2O_3, J. Magn. Magn. Mater. 41 (1984) 75-78.

[13] W.F.F.W. Ali, M. Othman, M.F. Ain, N.S. Abdullah, Z.A. Ahmad, The behavior of high frequency tunable dielectric resonator antenna (DRA) with the addition of excess Fe_2O_3 in $Y_3Fe_5O_{12}$ (YIG) formulation, J. Mater. Sci-Mater. El. 25 (2014) 560-572.

[14] W.F.F.W. Ali, M. Othman, M.F. Ain, N.S. Abdullah, Z.A. Ahmad, Studies on the formation of yttrium iron garnet (YIG) through stoichiometry modification prepared by conventional solid-state method, J. Eur. Ceram. Soc. 33 (2013) 1317-1324.

[15] X. Li, J. Zhou, J. Deng, H. Zheng, L. Zheng, P. Zheng, H. Qin, Synthesis of Dense, Fine-Grained YIG Ceramics by Two-Step Sintering, J. Electron. Mater. 45 (2016) 4973-4978.

[16] F. Chen, Q. Li, X. Wang, J. Ouyang, Y. Nie, Z. Feng, R. Gong, Y. Chen, V.G. Harris, Crystal structure tailored microwave magnetodielectric in $Yb_xY_{3-x}Fe_5O_{12}$ ceramics, J. Alloy. Compd. 726 (2017) 1030-1039.

[17] Vapor Pressure of the Metallic Elements, in: David R. Lide (Eds.), CRC Handbook of Chemistry and Physics, 84th Edition, online version. CRC Press. Boca Raton, Florida, 2003.

[18] W.F.F.W. Ali, M. Othman, M.F. Ain, N.S. Abdullah, Z.A. Ahmad, Sintering and grain growth control of high dense YIG, Ceram. Int. 42 (2016) 13996-14005.

[19] M.N. Rahaman, ceramic processing and sintering, 2nd ed. M. Dekker Inc. New York, 2003.

[20] P.B.A. Fechine, E.N. Silva, A.S. de Menezes, J. Derov, J.W. Stewart, A.J. Drehman, I.F. Vasconcelos, A.P. Ayala, L.P. Cardoso, A.S.B. Sombra, Synthesis, Structure and Vibrational Properties of GdIGx:YIG1-X Ferrimagnetic Ceramic Composite, J. Phys. Chem. Sol. 70 (2009) 202-209.

[21] Wu, H., Liu, J., Liang, H., & Zang, D. (2020). Sandwich-like Fe3O4/Fe3S4 composites for electromagnetic wave absorption. Chemical Engineering Journal, 393(March), 124743.

[22] Zou, J., Wang, Z., Yan, M., & Bi, H. (2014). Enhanced interfacial polarization relaxation effect on microwave absorption properties of submicron-sized hollow Fe3O4 hemispheres. Journal of Physics D: Applied Physics, 47(27).

[23] Lan, D., Qin, M., Yang, R., Chen, S., Wu, H., Fan, Y., Fu, Q., & Zhang, F. (2019). Facile synthesis of hierarchical chrysanthemum-like copper cobaltate-copper oxide composites for enhanced microwave absorption performance. Journal of Colloid and Interface Science, 533, 481–491.

Figures

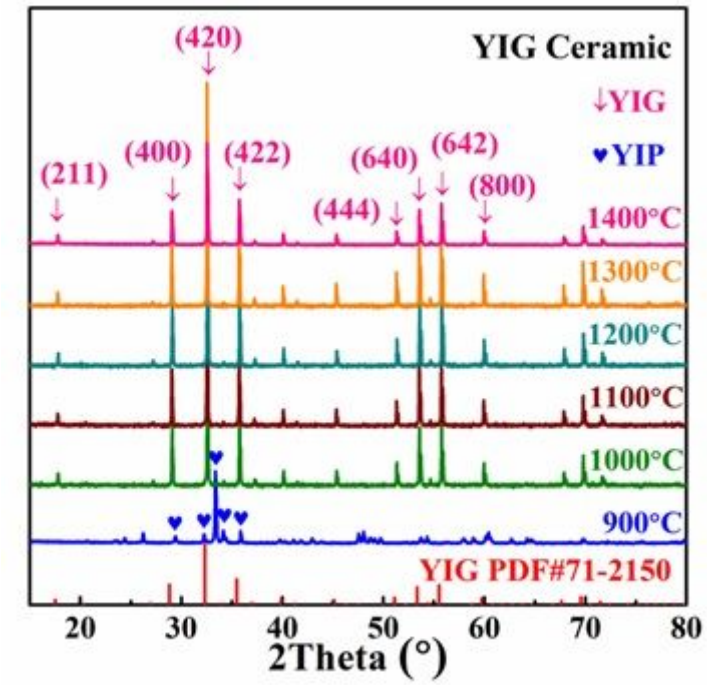

Figure 1

The XRD patterns of YIG ceramics sintered under various temperatures in air atmosphere.

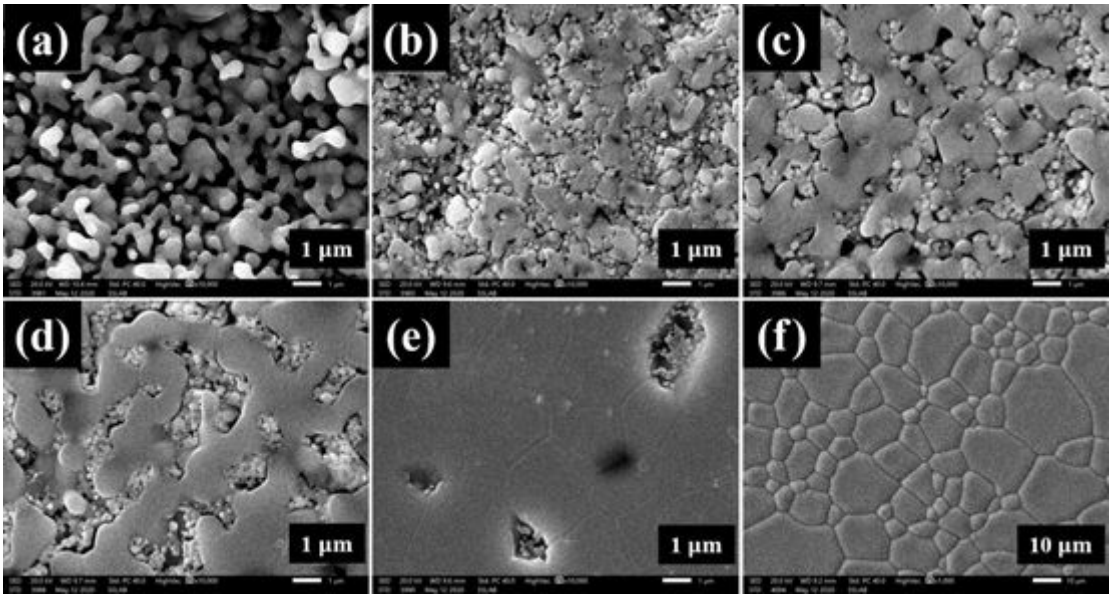

Figure 2

SEM images of YIG ceramics sintered at (a) 900 □, (b) 1000 □, (c) 1100 □, (d) 1200 □, (e) 1300 □ and (f) 1400 □ for 10 h.

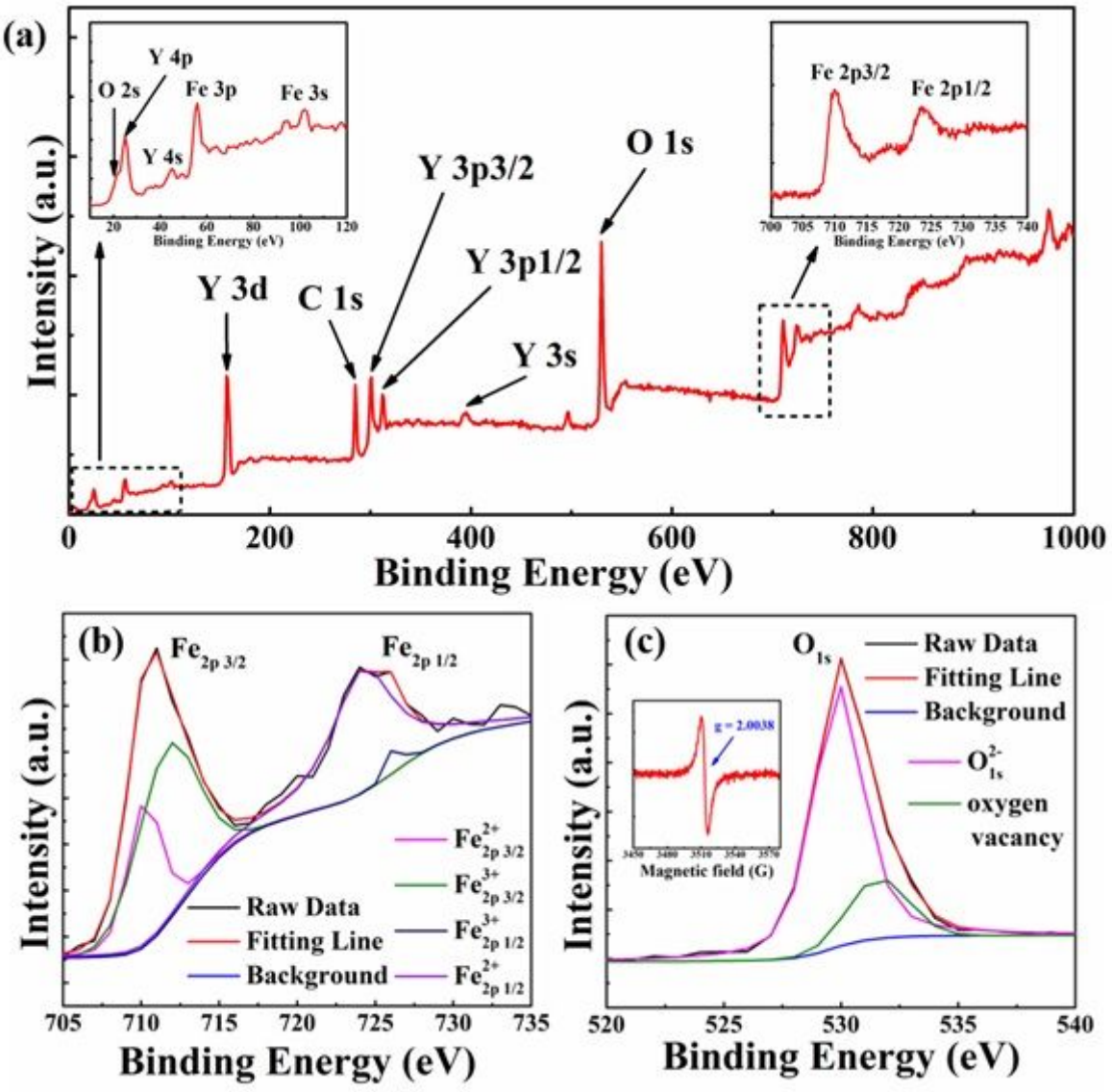

Figure 3

XPS spectra in (a) the survey range, (b) Fe ion and (c) O ion in YIG ceramics sintered at 1400 ℃ for 10 h.

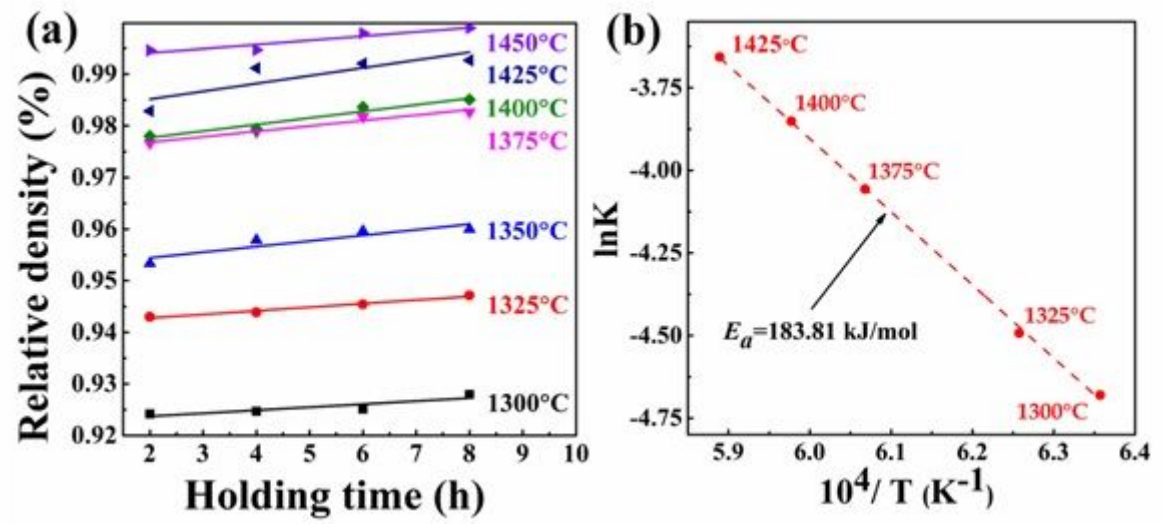

Figure 4

(a) Relative densities of YIG ceramics sintered at various temperatures and holding times. (b) The activation energy analysis for YIG ceramics.

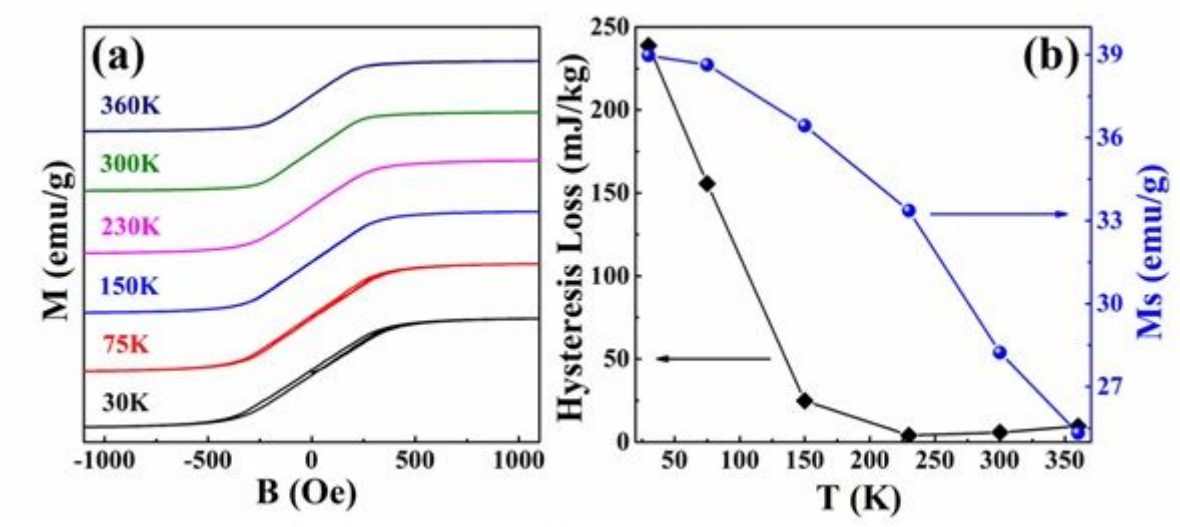

Figure 5

(a) Magnetic hysteresis loops and (b) Ms and hysteresis loss of YIG ceramics sintered at 1400 ºC for 8 h at various test temperatures.

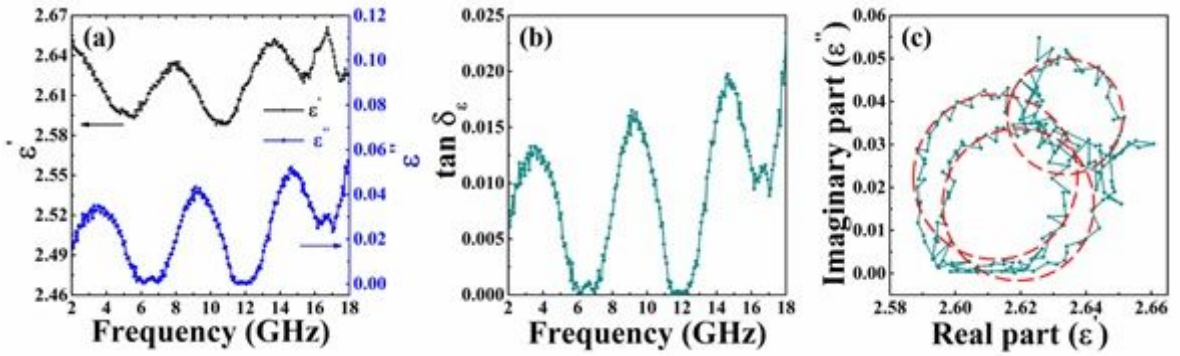

Figure 6

Frequency dependence of (a) ε^' and ε^", (b) tanδ_ε, and (c) Cole-cole semicircle of YIG ceramics sintered at 1400 ºC for 8 h.

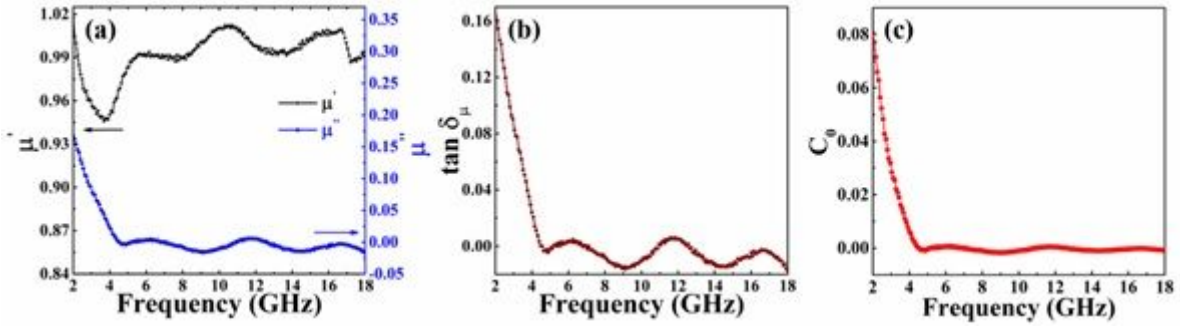

Figure 7

Frequency dependence of (a) μ^' and μ^", (b) tanδ_μ, (c) C0 of YIG ceramics sintered at 1400 ºC for 8 h.